

Vyacheslav F. BEZYAZYCHNY*, Marian SZCZEREK**, Mikhail V. TIMOFEEV***,
Roman V. LYUBIMOV****

FRETTING CORROSION EFFECT ON FATIGUE RESISTANCE OF GAS TURBINE ENGINE PART MATERIAL

WPLYW KOROZJI CIERNEJ NA WYTRZYMAŁOŚĆ ZMĘCZENIOWĄ MATERIAŁU CZĘŚCI SILNIKA TURBINY GAZOWEJ

Key words:	fretting corrosion, material fatigue: high-cycle, low-cycle, fatigue enhancement, surface plastic deformation methods.
Abstract:	The paper presents the results of a study on the fretting corrosion effect on strength as per the diagrams of material fatigue of low-cycle and high-cycle loading. An experimental study of the effect of fretting corrosion on fatigue of a titanium alloy VT3-1 showed that, when choosing a particular technological method to increase fatigue resistance of gas turbine engine parts operating under fretting corrosion conditions, it is necessary to take into account the fact that fretting itself is intensive strengthening and at the same time a softening factor affecting the surface layers of the material. Technological methods of surface plastic deformation treatment result in a significant change in the parameters of metal surface layer state, which depends on both the type and duration of treatment. If the power and time parameters of processing are too high, the surface may be re-cold worked and the surface layer of the material almost completely exhausts the reserve of plasticity, as a result dangerous microcracks occur, and the formation of particles of flaking metal emerge. Possible ways using technological methods have been suggested by the authors to improve fretting strength of part surfaces operating under fretting corrosion conditions.
Słowa kluczowe:	korozja cierna, zmęczenie materiału, wysoka częstotliwość, niska częstotliwość, zwiększanie odporności na zmęczenie, metody odkształcania plastycznego powierzchni.
Streszczenie:	W artykule przedstawiono wyniki badań wpływu korozji cierniej na wytrzymałość zmęczeniową przy niskiej i wysokiej częstotliwości obciążania. Eksperymentalne badania wpływu korozji cierniej na zmęczenie stopu tytanu VT3-1 wykazały, że wybierając metodę technologicznego zwiększania odporności zmęczeniowej części silników turbogazowych pracujących w warunkach korozji cierniej, należy wziąć pod uwagę fakt, że sam fretting jest czynnikiem wzmacniającym i jednocześnie osłabiającym warstwy wierzchnie materiału. Technologiczne metody powierzchniowej obróbki plastycznej powodują istotną zmianę parametrów stanu warstwy metalu w zależności zarówno od rodzaju, jak i czasu trwania obróbki. Gdy parametry obróbki (moc i czas) są zbyt duże, powierzchnia zostaje poddana obróbce na zimno, warstwa wierzchnia materiału nie jest podatna na odkształcenie plastyczne, wobec czego powstają niebezpieczne mikropęknięcia oraz tworzą się odpryski. Wskazano potencjalne zabiegi technologiczne rekomendowane do zwiększenia odporności elementów maszyn pracujących w warunkach występowania korozji cierniej.

INTRODUCTION

The intensity of the effect of metal fatigue strength due to fretting corrosion depends on many factors. However, the number of fretting corrosion cycles becomes the

determining factor for aircraft engine parts, since the other factors are regulated in one way or another by the design and operating conditions of real gas turbine engine designs.

* ORCID: 0000-0002-7287-2495. P.A. Solovyov Rybinsk State Aviation Technical University (152934, Rybinsk, Yaroslavl region), Pushkin Street 53, Russia, e-mail: technology@rsatu.ru.

** ORCID: 0000-0002-1049-7853. Łukasiewicz Research Network – Institute for Sustainable Technologies, Pułaskiego 6/10 Street, 26-600 Radom, Poland.

*** ORCID: 0000-0003-4480-7220. P.A. Solovyov Rybinsk State Aviation Technical University (152934, Rybinsk, Yaroslavl region), Pushkin Street 53, Russia.

**** PJSC “UEC-Saturn”, Rybinsk, Russia.

Analysis of operating conditions and causes of the destruction of disks of GTE low-pressure compressor second stage selected as the object research has shown that this gas turbine engine unit requires scientific substantiated approach to the choice of design and technological measures to ensure the required cyclic durability. Despite the fact that the destruction of disks occurs as per the mechanism of low-cycle fatigue, in this work, an attempt was made to obtain more detailed information about the effect of fretting corrosion on both the low-cycle and high-cycle fatigue of the structural and technological model of the selected object.

EXPERIMENTAL STUDY OF EFFECT OF FRETTING DAMAGES ON HIGH-CYCLE FATIGUE OF TITANIUM ALLOY VT3-1

When working on the experiment methodology, the following main points were implemented:

1. Ambient temperature $\theta = 288$ K.
2. Displacement amplitude $A = 100$ μm , frequency $f = 30$ Hz, contact pressure $p_{\text{H}} = 5$ MPa.
3. The study was carried out on the special specimens made of VT3-1 and L70 alloys.
4. The parameters of the state of the specimen surface layer prior to the experiment corresponded to the technical conditions for disk manufacture applying special finishing operations.
5. The study was accomplished on the single-factor experiment principle using the combined method. Special specimens that were preliminarily damaged by fretting corrosion with different running hours were tested for fatigue prior to destruction of each specimen.
6. The duration of the continuous run for fretting wear of specimens was determined based on a previously obtained fretting wear diagram of this pair of materials for reasons of the reliable achievement of each of the three main stages of the process (adhesion interaction, run-in, steady wear).
7. The influence of the structural and technological stress concentrator in the form of a chamfered circular hole on fatigue of VT3-1 alloy under the simultaneous influence of fretting corrosion was studied.

The design of the special specimens made of VT3-1 alloy for conducting comparative tests for high-cycle fatigue is shown in **Fig. 1**. The design of L70 alloy counter-pieces used to create fretting corrosion damage in laboratory conditions is shown in **Fig. 2**.

The method of conducting the experiment was as follows. Special specimens (**Fig. 1**) totalling 20 pieces were divided into four structural and technological groups: specimens without a hole and fretting-corrosion damage (the initial state); specimens with a $\varnothing 3$ mm hole without fretting corrosion damages; specimens without a $\varnothing 3$ mm hole with fretting corrosion damages

of different run; specimens with a $\varnothing 3$ mm hole, and fretting corrosion damages of a different run.

Prior to the experiment all specimens were subjected to recrystallization annealing in the protective atmosphere ($T_{\text{ann}} = 650$ C) and were instrumented with strain gages with a gage length of $l = 10$ mm. In order to determine the necessary continuous run of specimen fretting wear to reliably achieve each of the 3 main stages of the fretting process, the fretting wear diagram for the specimen pair VT3-1-L70 was taken at the load parameters set above.

It is established that the end of the adhesion interaction stage corresponds to $N = 5 \cdot 10^4$ cycles, and the end of the run-in stage and the onset of the stage of steady wear corresponds to $N \approx 10^5$ cycles of interaction. Results of comparative tests for fatigue based on $N_0 = 5 \cdot 10^6$ cycles are presented in **Table 1**.

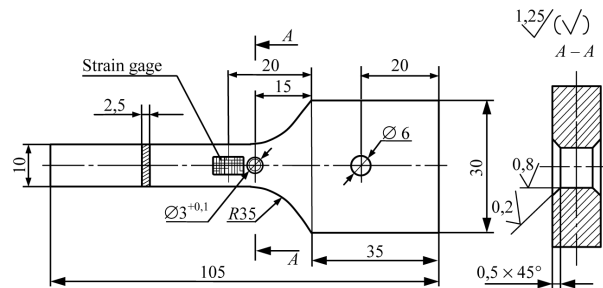


Fig. 1. Outline drawing of the specimen for conducting comparative tests for high-cycle fatigue (Split image A-A is enlarged 5-fold)

Rys. 1. Szkic próbki do przeprowadzenia testów porównawczych zmęczenia w wysokiej częstotliwości (fragment A-A jest powiększony 5-krotnie)

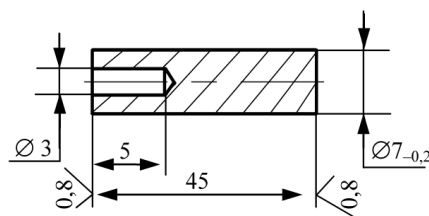


Fig. 2. Outline drawing of the counter-piece to produce fretting corrosion damages

Rys. 2. Szkic przeciwpróbki do badania zużycia w wyniku korozji czarnej

Table 1 indicates that fretting-corrosion damages of the surface, including those in conjunction with the structural and technological stress concentrator in the form of a circular chamfered hole, practically do not affect the high-cycle fatigue of the titanium alloy VT3-1. Indeed, comparing the obtained values of $\sigma_{-1}^{\text{cond}}$ in Groups 1 and 3, it is easy to see that decrease in endurance limit of specimens with fretting wear damage makes

Table 1. Specimen fatigue test results

Tabela 1. Wyniki testu zmęczeniowego próbeki

Group No.	Specimen No.	Conventional endurance limit: σ_{-1}^{cond} , MPa	Average value σ_{-1}^{cond} , MPa	Specimen rupture life N_{rupt} , tsd cycles
1	1.1	460	498	3301
	1.2	480		1130
	1.3	540		751
	1.4	510		975
	1.5	500		2066
2	2.1	310	306	950
	2.2	320		535
	2.3	300		880
	2.4	310		620
	2.5	290		1250
3	3.1	340	428	1183
	3.2	380		1500
	3.3	460		4600
	3.4	460		750
	3.5	500		747
4	4.1	260	294	539
	4.2	300		733
	4.3	300		464
	4.4	300		1640
	4.5	310		656

up $\Delta\sigma_{-1}^{cond} \approx 15\%$ relative to the original ones, which is commensurable with the statistical error of the experiment. At the same time, for Groups 1 and 4, the

value $\Delta\sigma_{-1}^{cond} \approx$ makes up 50%, and for Groups 1 and 2, $\Delta\sigma_{-1}^{cond} \approx -40\%$. To analyse and explain the data obtained, let us consider **Figure 3**.

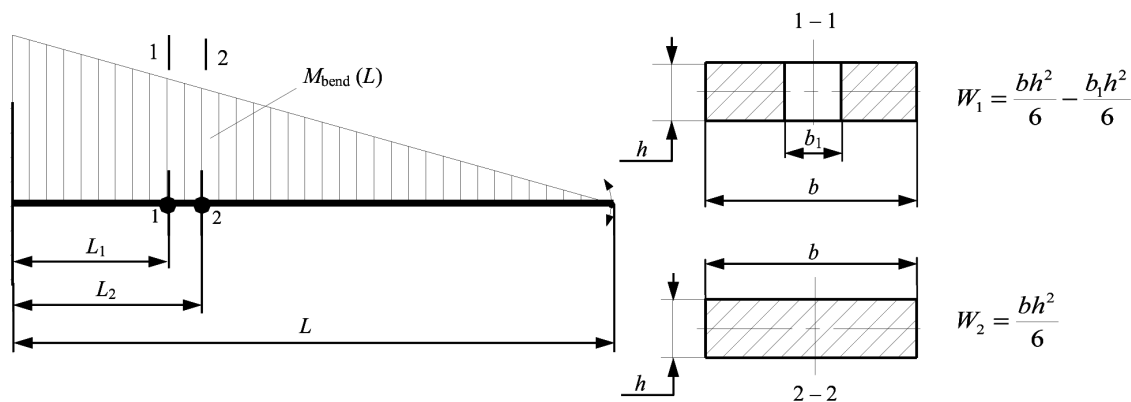


Fig. 3. Specimen loading diagram in the course of vibration testing for high-cycle fatigue

Rys. 3. Przykładowy schemat obciążenia w trakcie badań zmęczeniowych dla wysokiej częstotliwości wibracji

It is known that, for the cantilevered specimen diagram implemented in the course of vibration fatigue tests, there is a linear distribution of bending moment M along the length of the specimen (**Fig. 3**). In this case, actual stress at each point of the specimen is $\sigma = \frac{M}{W}$, where W is the moment of inertia of the cross-section of the specimen, m^3 .

Let us consider the stress state at Point 1 being the dangerous cross section of the sample with a hole of $\varnothing 3$ mm and Point 2 which is the place where the strain gage is attached and the actual stress amplitude is measured. Assuming that the values of the bending moment at Points 1 and 2 are approximately equal due to the fact that $L_1 \approx L_2$, we can calculate the value of the actual stress at point 1 at a known value of σ_2 :

$$\frac{\sigma_1}{\sigma_2} = \frac{M_1 \cdot W_2}{M_2 \cdot W_1} \Rightarrow \sigma_1 = \sigma_2 \cdot \frac{W_2}{W_1}.$$

At the same time, **Fig. 3** shows that $W_1 \neq W_2$ also at the existing geometric dimensions of the special specimen with a hole (**Fig. 1**): $W_1 \approx 2/3 W_2$. Then, $\sigma_1 \approx 1.5 \sigma_2$.

Thus, for specimens with a hole of $\varnothing 3$ mm, the value of the actual stress in the dangerous section (Point 1) is greater than that measured using the strain gage at Point 2. In this case, the values for Groups 2 and 4 will make up $\bar{\sigma}_{-1}^{\text{cond}}$ 460 and 441 MPa, respectively. The resulting picture of changes in various structural and technological groups of specimens $\bar{\sigma}_{-1}^{\text{cond}}$ (**Table 1**) gives reasons to assert that fretting-corrosion damages of the surface have a negligible effect on the high-cycle fatigue of VT3-1 alloy under the selected experimental conditions. Besides, the fractographic analysis of the fracture surface of specimens conducted applying instrumental microscope IMCL 150 \times 50.6 revealed that places of nucleation of fatigue hairline cracks characterized by presence of visible boundary step change of fatigue striations do not always correspond to the places of fretting corrosion surface damage. In some cases, fatigue cracks developed from the edge of specimens.

However, it should be noted that, on all the specimens both with a hole and without it having fretting corrosion damages with run $N \approx 2,5 \cdot 10^4$ cycles and $N \approx 510^4$ cycles (the stage of adhesion interaction), the fatigue nucleus was located in the immediate vicinity of surface damages, similar to destruction of disks. Moreover, just at these values of fretting wear duration, the minimum values of $\bar{\sigma}_{-1}^{\text{cond}}$ of the specimens were obtained in Groups 2 and 4 (**Table 1**).

The results obtained are in good agreement with the data of previous studies that the strongest influence of fretting corrosion on the fatigue resistance of metals is manifested at the stage of the adhesion interaction of the

contact surfaces. At the same time, the chosen method of conducting the experiment, consisting in the sequential effect of fretting and vibration fatigue loads, allowed evaluating the effect of fretting-corrosion damage on $\bar{\sigma}_{-1}^{\text{cond}}$ of titanium alloy VT3-1, but also in the presence of the stress concentrator in the form of a circular hole. The data obtained are in good agreement with the results published in [**L. 1, 2**].

EXPERIMENTAL STUDY OF EFFECT OF FRETTING CORROSION ON LOW-CYCLE FATIGUE OF TITANIUM ALLOY VT3-1

As known, there is a conditional division of the concept of metal fatigue into the high-cycle and the low-cycle ones. In this case, as a rule, the low-cycle fatigue changes in a wider range for specific parts of gas turbine engines when various external structural and technological factors are applied. First of all, this is due to transition to the elastic-plastic nature of the stress state of the material, when cyclic loads cause irreversible plastic deformation of the part material, upon reaching the level of actual stresses of actual yield point (σ_c^f). In this case, the actual yield strength should be understood as the minimum stress level at which irreversible changes in the crystal structure of the material occur, associated with increase in the number of dislocations, when reaching the critical density of which fatigue cracks begin to nucleate [**L. 3**]. It should also be noted that value σ_c^f is always less than the technical yield strength of the material ($\sigma_{0.2}$) and increases with accumulation of plastic deformation in the material.

The probability of the occurrence of stresses $\sigma \geq \sigma_c^f$ in the surface layer of the material of gas turbine engine parts increases under the influence of various structural, technological, and operational factors that change over time. Therefore, in design calculations of the cyclic durability of real parts, for example, the disks of an aircraft engine low-pressure compressor, the results obtained are used with the condition of a 5-fold margin, since they have a very uncertain probability boundary. However, as practice shows, low-cycle fatigue of disks changes even more widely, due to occurrence of an operational factor which was not subject to the calculations, i.e. fretting corrosion damages of the flanges.

Preliminary measurements of the residual stresses of the hardened and non-hardened specimens made of titanium alloy VT3-1 showed that the non-hardened edges have unstable residual stresses ranging from plus 8.9 to minus 25 MPa. At the same time, the use of strengthening treatment with glass balls $d = 0.15 \dots 0.20$ mm allows obtaining stable residual stresses up to minus 95.5 MPa with a depth of up to 120 μm . The latter circumstance should help to reduce the probability of disclosure and the progressive growth of fatigue microcracks, which inevitably occur in places of fretting-

corrosion damages. However, the comparative tests of hardened and non-hardened edges for cyclic durability carried out at the next stage give an ambiguous idea of effectiveness of this technological method to increase fatigue resistance of disks.

The method of conducting comparative tests of flanges for cyclic durability was as follows. From the maintenance disks of the IInd stage low pressure compressor having operating time $T = 7000\text{--}12000$ hours, special specimens were made representing flange fragments with one-side groove at one of the holes designed for the pin hinge of the rotor blade to the disk, as shown in **Fig. 4**.

Then, the surface of the specimens was strengthened by blasting with quartz glass balls on a pneumatic blasting machine for 6 minutes (3 minutes on each side). Then comparative tests of hardened and non-hardened specimens for cyclic durability were performed. The pre-calculated parameters of the cyclic loading of the specimens corresponded to the stress state of the disk edges when the engine was running at the rated mode. Some test results are presented in **Table 2**.

Analysing the experimental data obtained, it is easy to see that surface hardening according to the proposed technological method does not result in an increase in the cyclic durability of VT3-1 titanium alloy in this design (**Fig. 4**). In some cases, there is even significant decrease in the N_c of the hardened specimens relative to the non-hardened ones. In any case, all the obtained values of N_c for flange specimens of the low-pressure compressor disks are 1.5–2 times less than the allowed value [N_c], taking into account the 5-fold margin.

The results presented in **Table 2** can be explained as follows: In the process of engine operation, the fretting corrosion damages of the flange discs of the IInd and IIIrd stages of the low pressure compressor are observed due to technological imperfections of the swivel assembly of the rotor blade with the disk. As the previously conducted research has shown, these are the fretting corrosion damages that cause a significant reduction in fatigue resistance of disks. In several cases, this resulted in non-localized destruction of the engine as a whole.

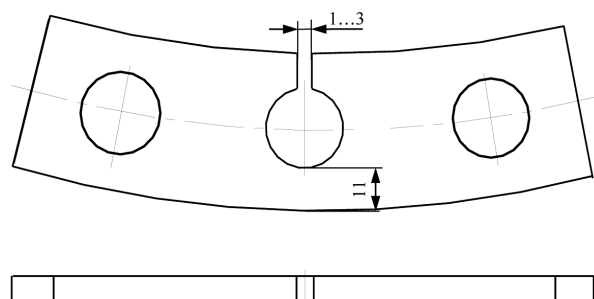


Fig. 4. Outline drawing of a specimen to conduct comparative tests for cyclic endurance

Rys. 4. Szkic przeciwpróbki do badań porównawczych trwałości zmęczeniowej

Table 2. Specimen comparative test results for cyclic endurance

Tabela 2. Wyniki badań porównawczych cyklicznej wytrzymałości próbek

Ser. No.	Surface layer state	Value of rupturing load P_{rupt} , N	Cyclic durability N_c , cycles
1	non-hardened	3500	100000
2	non-hardened	3580	35552
3	non-hardened	3500	43930
4	non-hardened	3500	70240
5	non-hardened	3500	61370
6	hardened	3500	38820
7	hardened	3500	96678
8	hardened	3450	65382
9	hardened	3500	53465
10	hardened	3500	67800

Meanwhile, the process of fretting wear of metals is accompanied by competing hardening-softening processes associated with the periodic accumulation of structural damage in thin surface layers of metals, followed by their destruction by the mechanism of low-cycle fatigue. In addition, fretting corrosion damages of the disk surface certainly act as a strong stress concentrator, which ultimately initiates the fatigue destruction of the material. For discs of the IInd and IIIrd stages of the low pressure compressor, the negative effect of fretting on fatigue life is enhanced due to the crystal lattice of titanium alloy VT3-1.

When strengthening the flanges, due to impact of glass balls on the surface layers of the material, additional strengthening occurs of the surface microvolumes pre-riveted during fretting, which results in the intensification of fatigue failure processes, since the surface layer of the material experiences the greatest stress when applying cyclic loads.

Thus, when choosing a particular technological method to increase fatigue resistance of gas turbine engine parts operating under fretting corrosion conditions, it is necessary to take into account the fact that fretting itself is intensive strengthening and, at the same time, a softening factor affecting the surface layers of the material. In this case, the latter circumstance did not allow obtaining the necessary increase in the cyclic durability of the disks of the IInd stage of the low-pressure compressor. At the same time, as will be shown below, it is possible to significantly increase the effectiveness of existing technological methods of surface plastic deformation (SPD) through the scientifically substantiated defining processing modes.

POSSIBILITIES OF THE APPLICATION OF MODERN TECHNOLOGICAL METHODS OF SURFACE PLASTIC DEFORMATION (SPD) TO IMPROVE THE PERFORMANCE PROPERTIES OF AIRCRAFT GAS TURBINE ENGINE PARTS.

Currently, in the manufacture of critical parts of machines operating under cyclic loads, various technological methods of SPD hardening are used to improve the performance properties of parts, primarily fatigue resistance, wear resistance, and contact stiffness. However, the creation of significant residual technological stresses in the surface layer of the material can adversely affect the performance of the part, since additional plastic deformation during friction and contact loads results in embrittlement of the surface layer [L. 4, 5, 6]. In this regard, there is a problem in choosing the optimal modes of hardening by SPD methods, as well as developing simple and effective methods for monitoring the parameters of the surface layer state after processing. In this case, a method to determine the modulus of elasticity of metal surface layers has proven itself positively in the study of kinetics of surface destruction of metals in the process of abrasive wear and fretting corrosion [L. 7].

The research methodology was as follows: The end faces of cylindrical specimens made of low-carbon steel 20 with a diameter of \varnothing 15 mm and a height of $h = 20$ mm were subjected to hardening by various SPD methods with different durations. The following technological methods of SPD hardening were studied:

1. Hardening with steel microballs (SHH15) on a pneumatic blasting machine (diameter of balls $d_b = 150$ μm , blasting time $T_{\text{blast}} = 3$ and 6 min);
2. Hardening with quartz glass balls on a pneumatic blasting machine (diameter of balls $d_b = 150$ μm , $T_{\text{blast}} = 3$ and 6 min);
3. Hardening with steel (SHH15) microballs on a hydro-blasting unit ($d_b = 180$ μm , $T_{\text{blast}} = 3$ and 6 min., distance to the nozzle $L = 150$ mm, pressure $P = 4$ atm);
4. Hardening with lead pellets on a pneumatic blasting machine ($d_{\text{pellet}} = 0.8 - 1.2$ mm, $T_{\text{blast}} = 3$ min, $L = 150$ mm, $P = 3.8$ atm).

Surface roughness Ra was measured before and after blasting with a Shapemeter B-245. The contact time of the elastic impact of the indenter with the specimen τ was measured using the method mentioned in [L. 9] under the following initial conditions: a spherical indenter made of SHH15 steel in the hardened and low-released state, the radius of the indenter is 7.5 mm with a mass of 0.014 kg, the height of the indenter drop is 3 mm, and the depth of elastic penetration of the indenter is ≈ 7 μm .

Microhardness H_0 of the surface layer with a depth of 1.5–7 μm was measured using a PMT-3 device at loads of 20, 50, 100, and 200 g prior to and after SPD

hardening. For differentiated assessment of the influence of the degree of plastic deformation and changes in microgeometry (roughness) of the surface layer on the behaviour of elastic modulus E , recrystallization annealing of specimens in a protective atmosphere was performed, followed by a control measurement τ , Ra , H_0 . It was found that roughness parameter Ra did not change after annealing.

In all experiments, the value τ is the result of averaging a series of 25...30 measurements, $Ra - 5...10$ measurements, and $H_0 - 10...15$ measurements. The relative error in determining the modulus of elasticity was 1–3% with confidence probability of 0.95. In addition to the contact time, the relative change in the elastic modulus was taken as the final result of the experiment $\Delta E / E = (E_{\text{chng}} - E) / E$.

Table 3 presents the following: measurement results τ related to the type and duration of SPD hardening; values corresponding to them $\Delta E / E$ ($\Delta E / E_{\text{max}}$), which are the maximal measured relative changes of the modulus of the surface layer; $\Delta E / E_{\text{def}}$, which are the changes in the surface layer modulus conditioned by plastic yield; $\Delta E / E_{\text{rough}} = \Delta E / E_{\text{max}} - \Delta E / E_{\text{def}}$ (which are the apparent changes in the surface layer modulus due to change in roughness), as well as the results of measuring microhardness H_0 under loads of 20, 50, 100, and 200 g (value \bar{H}_0 corresponds with the average value of microhardness under the relevant load).

Analysis of the experimental data obtained permitted us to deduce the following:

1. Technological methods of SPD treatment result in a significant change in the parameters of steel surface layer state: the elasticity modulus of the material of the surface layer decreases, and the value $\Delta E / E$ depends on both the type and duration of treatment; and, the roughness of the treated surface is significantly higher than that of the untreated one.
2. The decrease in the elasticity modulus of the treated surface material in relation to the conditionally undeformed surface material is primarily due to the avalanche-like development of dislocations that accumulate near the shear lines, and their subsequent inhibition before various kinds of obstacles which are formed in the process of plastic deformation or those which existed prior to it.
3. If the power and time parameters of processing are too high, the surface may be re-cold worked. Thus, when hardening according to option 1, there is reason to assert that the surface layer of the material almost completely exhausts the reserve of plasticity. Relative changes in the modulus of elasticity due to plastic deformation after processing as per this variant were 17.8 and 19.6 %, respectively, for 3 and 6 minutes of processing (**Table 3**). At the same time, it is known that the ratio $(E / E) \approx 30\%$ corresponds to the extremely deformed state of the surface layer, as a result of which dangerous microcracks occur,

and the formation of particles of flaking metal emerge [L. 8–9].

4. Cold working of the metal can be partially or completely removed by recrystallization annealing. In this case, this allowed separating effects of the degree of plastic deformation and changes in surface roughness on the relative change in the elasticity modulus. It should be noted that local heating, which is accompanied by plastic deformation, also reduces the effect of the hardening of thin surface layers and causes the zone of its maximum value to shift to the subsurface layer. Softening caused by the breakdown of martensite grows with increasing processing time.
5. Due to SPD treatment, there is significant increase in surface roughness relative to the original one. In this case, roughness parameter Ra increases by an average of 1–2 μm during shot blasting of the ground surface of steel. This is also explained by processes of plastic deformation, when the micro-volumes of the surface layer of the material are redistributed and a new roughness structure is formed, which different from the original one.

Table 3. Results of measuring parameters of steel 20 specimen surface layer depending on the type and duration of SPD hardening

Tabela 3. Wyniki pomiaru parametrów warstwy wierzchniej próbki stali 20 w zależności od rodzaju i czasu trwania hartowania SPD

Type of SPD treatment	Surface roughness		Contact time τ_{chg} , μs	Contact time τ_{ann} , μs	Relative change of elasticity modulus, $\Delta E/E$, %			Microhardness H_0 , MPa under load				
	T_{blast}^* , min	\bar{R}_a , μm			$\Delta E/E_{\text{max}}$	$\Delta E/E_{\text{def}}$	$\Delta E/E_{\text{rough}}$	20 g	50 g	100 g	200 g	\bar{H}_0
1	3	2.23	75.3	70.4	23.6	17.8	5.8	220	306	354	362	341
	*	0.7	68.6	68.9	—	—	—	200	200	200	200	200
1	6	1.91	77.1	71.7	29.8	19.6	10.2	220	336	294	321	317
	*	0.67	68.7	69.2	—	—	—	200	200	200	200	200
2	3	0.89	69.2	69.0	5.1	0.7	4.4	207	249	270	283	267
	*	0.65	68.0	68.0	—	—	—	200	200	200	200	200
2	6	1.0	71.0	69.8	118	4.4	7.4	200	223	254	261	246
	*	0.65	68.0	67.6	—	—	—	200	200	200	200	200
3	3	2.0	71.7	70.2	13.9	5.6	8.8	207	274	325	308	302
	*	0.55	68.7	66.8	—	—	—	200	200	200	200	200
3	6	2.42	72.3	71.6	14.4	6.1	7.8	216	249	309	325	294
	*	0.57	69.8	67.2	—	—	—	200	200	200	200	200
4	3	2.9	73.0	70.7	18.8	8.5	10.3	203	289	272	271	277
	*	0.65	68.2	67.6	—	—	—	200	200	200	200	200

* Initial specimen without processing.

CONCLUSIONS

Based on the above, it can be concluded that degree and depth of SPD hardening due to plastic deformation of the surface layer is directly related to the increase in the number and density of dislocations, vacancies, and other defects in the crystal structure of the material. At the same time, application of different types of SPD results in different degrees of hardening of the surface layer at the same processing time. In this case, the most “soft” effect on the surface layers of steel was obtained by hardening Variant 2: $\Delta E/E_{\text{surf}}$, which was 1.4 and 8.8%, respectively, for 3 and 6 minutes of processing. In addition, this type of processing results in minimal change in the initial surface roughness. In this sense, Methods 3 and 4 also showed the positive results, for which the value of $\Delta E/E_{\text{surf}}$ does not exceed 20%, i.e. it does not approach the critical value.

As for the dynamics of changes in the microhardness H_0 in the depth of the surface layer, it should be noted that all the presented technological SPD methods assume a stable increase in compressive

residual stresses at a depth of $\approx 7 \mu\text{m}$ from the surface of the material with degree of hardening of 30–60%. The latter circumstances are the advantage of SPD in relation to other technological methods for ensuring the specified quality parameters of the surface layer of gas turbine engine parts and provide increase in wear resistance, fatigue resistance, contact stiffness, and other performance properties by 20–50%, and in some cases – 2–3-fold (provided that the optimal parameters of SPD have been selected). However, the results of comparative tests for cyclic durability suggest that these performance properties are increased only to a certain degree of hardening, exceeding of which results in the opposite effect.

From the point of view of the task of choosing the optimal conditions for SPD hardening, the data obtained by the authors are of great practical interest and are in good agreement with the previous research in the field of surface processing. It allows choosing the correct method of surface hardening and its execution mode in order to ensure the required level of fretting resistance of the surface.

REFERENCES

1. ASM Handbook, “Corrosion” Vol. 13, ASM International, 1987.
2. Fenner A.J., Field J.E.: A study of the onset of fatigue damage due to fretting. North East Coast Inst. of Eng. and Shipbuilders. 76, 4, 183, 1960.
3. Bezyazychny V.F., Drapkin B.M., Osadchy N.V.: Investigation of elastic characteristics and internal friction under bending vibrations of cantilevered samples, Problems of strength, 1997, No. 12, pp. 46–52.
4. Marchenko E.A.: On the nature of metal surface destruction under friction, Nauka, 1979, p. 118.
5. Marchenko E.A., Nepomnyashchiy E.F., Kharach G.M.: Cyclical nature of phase distortion accumulation in the surface layer as physical verification of fatigue nature of wear, DAS, USSR, 1968, V. 181, pp. 1103–1104.
6. Pinchuk V.G., Andreev S.F.: Kinetics of hardening and destruction of metal surface layer under contact loading, Modern issues of mechanical engineering, Proceedings of the ISTE, Gomel, 1996, pp. 57–59.
7. Bezyazychny V.F., Drapkin B.M., Kiselev E.V., Kononenko V.K., Timofeev M.V.: Measuring system for determining physical and mechanical characteristics of materials, Monitoring. Diagnostics, 1999, No. 2, pp. 17–22.
8. Bezyazychny V.F., Drapkin B.M., Lyubimov R.V.: Establishment of the operational properties of friction couples parts in accordance with the parameters of the surface layer. Crakow, Poland, PROBLEMY EKSPLOATACJI, No. 3, 1998, pp. 29–40.
9. Bezyazychny V.F., Drapkin B.M., Lyubimov R.V.: Investigation of behavior of the elasticity modulus of metal surface layers under abrasive force impact, Inter-university collection of scientific papers “Mechanics and physics of friction contact”, Tver, 1998, pp. 50–60.
10. Bezyazychny V.F., Drapkin B.M., Lyubimov R.V.: Investigation of elastic and dissipative properties of surface layers of metal materials under abrasive force impact. Dep. in All-Union Institute of Scientific and Technical Information on 17.02.98, No. 483-B98, p. 14.